Journal of Polymer Research (2022) 29: 131
https://doi.org/10.1007/s10965-022-02966-y

ORIGINAL PAPER

Mechanical, viscoelastic and gas transport behaviour of rotationally molded polyethylene composites with hard- and soft-wood natural fibres

K. Prasad[1] · **M. Nikzad**[1] · **I. Sbarski**[1]

Received: 2 December 2021 / Accepted: 1 March 2022 / Published online: 15 March 2022

Abstract
Rotomolded uncompatibilized composites of LLDPE with softwood and hardwood flour dispersed phases are compared and contrasted with respect to their static (tensile, flexural and impact) and dynamic (creep modelling, storage and loss moduli) mechanical properties and transport (oxygen permeability). The static and dynamic mechanical properties are analysed as a function of dispersed phase weight fraction and pre and post ethanol sorption. Vital structural properties such as the equilibrium modulus, Kelvin Voigt modulus, Kelvin Voigt viscosity and relaxation times along with creep compliance trends are analysed. The interfacial porosity generated is then correlated to the overall gas transport using oxygen as the probe molecule. Two models are compared and it is found that the model of Alter which uses overall density as the modelling parameter, is able to predict composite gas permeability with high accuracy. Overall, owing to the uncompatibilized nature, most mechanical properties reduce with wood flour incorporation independent of the type of dispersed phase. However, these properties remain consistent pre and post ethanol sorption as long as the dispersed phase weight fraction is around 5%. This indicates that with some external scaffolding type support structures, the rotomolded composites have potential for use as storage units for liquid materials.

Keywords Composites · Packaging · Mechanical properties · Gas permeability modelling · Viscosity and viscoelasticity

Introduction

Rotational molding or Rotomolding is one of the fastest growing polymer processing techniques and is highly suitable for the manufacture of large volume (> 2 m^3) polymeric storage units. The process of rotomolding consists of 4 basic steps viz., charging, rotation + heating, cooling and demolding. Due to the relative simplicity of the process, rotomolding has very few competitors for the production of large (> 2 m^3) hollow objects in one piece [1]. The products fabricated using rotomolding find application in a wide spectrum of industries ranging from agriculture to the automotive sector [1–4]. The specific polymers that may be rotomolded include polyolefins (High density Polyethylene- HDPE, linear low density polyethylene- LLDPE, linear medium density polyethylene- LMDPE, low density polyethylene- LDPE) [1–4]), Polypropylene (PP), Polycarbonate (PC), Polyamides (PA), Polyurethanes (PU), Poly (vinyl chloride)- PVC, Acrylonitrile–Butadiene–Styrene (ABS) terpolymer, High Impact Polystyrene (HIPS), various fluoropolymers, liquids such as liquid Nylon block copolymer, liquid polyurethanes, and recently, biodegradable plastics like Poly (lactic acid)- PLA and foamed plastic analogues of the polymers already mentioned [1–4].

Polymer natural fiber composites are now being increasingly used for applications in construction, packaging, and automotive industries. Detailed work on the nature and properties of polymer-natural fibre composites can be seen in [5–13] and in these works, the advantages provided by the incorporation of natural fibres in polymers are established. These include low cost, low density (good specific properties), reduced wear in processing equipment, high toughness, biodegradability, and ecological friendliness. As far as the rotomolding of polymer composites are concerned, a review of some of the work is shown in Table 1.

✉ K. Prasad
krishnamurthyprasad@swin.edu.au

[1] Faculty of Science, Engineering and Technology, Swinburne University of Technology, John Street, Hawthorn, VIC 3122, Australia

Table 1 Review of mechanical properties of rotomolded polymer natural fibre composites

Composite system		Results	Reference
Polymer	**Fibre**		
HDPE	Sisal, Cabuya	Overall reduction in impact energy due to fiber addition. 55% reduction at 7.5% sisal loading and 33% reduction at 6% cabuya loading. Tensile strength remains consistent	[14]
LLDPE	Flax	A slight increase in both impact energy (3%) and in tensile strength (6%) was seen at 10% loading of fibre. This is attributed to improved dispersion of fibre owing to dicumyl peroxide surface treatment	[15]
LMDPE	Agave	The addition of agave fibers in PE and consequent rotomolding resulted in a product with increased flexural and tensile moduli but there was a reduction in impact strength, as well as tensile and flexural strengths The optimum fiber concentration is around 10% based on the difficulty of the polymer matrix to completely wet all the fibers in excess to 10%	[16]
LMDPE	Sisal	Tensile strengths showed a steady decrease with increasing fibre content for both sisal-LMDPE and wood fibre-LMDPE composites, tensile moduli generally increased with increasing fibre content up to 15 wt% for both sisal-LMDPE and wood fibre-LMDPE composites The driving force behind the adverse effects on the mechanical properties were fibre agglomeration and the shorter fibre lengths	[17]
LLDPE	Maple	Treatment of the maple fibres by maleic anhydride grafted polyethylene and consequent dispersion into the LLDPE matrix via rotomolding resulted in composites with superior mechanical properties as compared to untreated fibres For 30% fibre incorporation, there was a 42% increase in flexural strength for untreated maple fibre LLDPE composites and a 60% for treated maple fibre LLDPE composites compared to plain LLDPE Microstructural analysis of the composites showed the presence of holes and voids. These holes/voids could be divided into in two categories: 1.Holes/voids produced by fibre debonding. The debonding holes result from fibre pull-out and are typical in composites with poor fibre wettability and adhesion 2.Holes/voids related to trapped air. This air is imprisoned between the powder particles due to incomplete sintering and/or gases released by the fibres themselves	[18]
PLA	Agave	Uptake of water in rotomolded composites was studied and it was found that the surface treatment (using maleic anhydride grafted PLA) of the Agave fibres lead to a reduction in diffusion coefficient and overall uptake Parameter based on density differential akin to Vp studied in Prasad et al. [19] was used to characterize the composite specimens 20% by weight of the treated agave fibres was found to be the optimal concentration. The tensile strength and modulus of treated fiber composites increased by up to 68% (from 25 to 41 MPa) and 32% (from 1.30 to 1.74 GPa) respectively, in comparison with untreated fiber composites at 20% incorporation	[20]
Metallocene PE	Banana Abaca	Increase in tensile and flexural moduli were observed for the composites. Simultaneous grinding of the metallocene PE and the fibres helped in dispersion prior to rotomolding However, impact strength reduced significantly with and without surface treatment of the fibres. This paper suggested that efficient dispersion of the untreated fibres was easier to achieve than for the treated fibres	[21]
Recycled PP	Lignocel C120 wood flour	Silanization based surface modification of the lignocellulosic fibres helped in reduction of wood flour particle size and assisted in efficient dispersion. The differences between measured composites densities and theoretical density confirmed the presence of porous microstructure similar to Gonzalez Lopez [11] for 5% by weight incorporation of treated and untreated wood fibre. A higher amount of the pores were seen for the composite filled with unmodified filler Unlike [18], there was a consistent drop in mechanical properties with or without compatibilization in [22]. Adding 5 weight % of untreated and treated wood fibre caused a 29% and a 40% respectively decrease of tensile strength in comparison with pure recycled PP	[22]

Table 1 (continued)

Composite system		Results	Reference
Polymer	**Fibre**		
PLA	Ficus	Reinforcement of the PLA matrix was observed when the modified ficus (2.3%, by weight corresponding to a volume fraction of 4.1%) was added The flexural modulus went up from 1.4 GPa (plain plasticized PLA) to 1.7 GPa, the flexural strength from 20 MPa (plain plasticized PLA) to 32 MPa and the toughness is increased from 0.40 (plain plasticized PLA) to 0.44 mJ/mm^3 The elongation at break, however, reduced from 2.9% (plain plasticized PLA) to 2.1%	[23]
LLDPE	Maple	While the results in [24] indicated that the effect of matrix particle size on the properties of rotomolded PLA is negligible, the work of Hanana [25] indicates that effect of dispersed phase particle size is highly significant The tensile modulus increased by 7%, 40%, and 73% for 125–250, 250–355, and 355–500 mm at 30 wt% of maple fibers. The tensile strength also increased by 114% at the same fiber loading (30 wt%) when the particle size increased from 125–250 mm to 355–500 mm The impact strength with 355–500 mm particles was 52% higher than for 125–250 mm particles at 30 wt%	[25]
LLDPE	Short coir fibre Coconut fibre	Plasma modification of LLDPE surface was conducted and used in combination with surface modification of the natural fibres to improve dispersibility for rotomolding. 4 different types of interfaces viz., PE/natural fibre, PE/bleached natural fibre, plasma modified PE/natural fibre, plasma modified PE/bleached natural fibre Among all, plasma modified PE/bleached natural fibre showed the best balance of properties. The plasma modified PE/bleached natural fibre composite showed a 122% higher tensile modulus and ~ 66% higher impact strength than pure PE	[26]

Thus, from the literature collected in Table 1, it can be seen that the rotationally molded polymer composites do show some reduction in mechanical properties compared to the virgin material. This can be improved by surface treatment of the wood fibre dispersed phase. The review of the literature indicates certain gaps and are addressed in this paper as follows:

1. A detailed comparison of the thermomechanical properties of rotomolded composites under dry and wet conditions is limited in the current literature. Therefore, the first set of results in this paper will cover the static properties of the rotomolded composites under wet and dry conditions for two types of dispersed phase, softwood pine flour and hardwood oak flour.
2. The long-term mechanical properties data reported for the rotomolded composites in literature is also limited. Only the works of Chandran and Waigonkar [25, 27] and Pozhil et al. [28] expound on this. In [25, 27] it is reported that the nature of the dispersed phase has a massive influence on the creep properties with an analytical model for the creep deformation shown in [28]. In our previous work, we presented the creep modelling for rotomolded LLDPE softwood (pine) composites under dry and wet conditions. It was found that with ethanol uptake, all rotomolded composites deteriorated mechanically at different rates. While 5% and 10% pine-based composites retained most of their properties similar to that of the plain rotomolded LLDPE, the 20% pine samples deteriorated significantly. As rotomolding is a conventional processing method used for manufacturing storage units, for any potential storage application, the pine incorporation could be optimized at 10% by weight in terms of the long-term properties. In order to see is similar trends are seen for a hardwood dispersed phase, the properties obtained for the optimised pine flour rotomolded composite (RM10) are compared with 5% and 10% by weight oak flour rotomolded composites. In addition, fitting a viscoelastic model (the Burger's model detailed in [29]) and determining critical structural parameters such as the equilibrium modulus, Kelvin Voigt modulus, Kelvin Voigt viscosity and relaxation time as a function of dispersed phase and ethanol uptake is conducted. This can then be compared and contrasted with the trends in Maxwell moduli and viscosities indicated in [29].
3. Thirdly, the V_P parameter covered in [19] and [29], which was correlated to ethanol diffusion in [29] is used in this paper to correlate to the overall gas transport phenomena. A more detailed correlation of interface and morphology with the transport (specifically, ethanol sorption) was also been conducted in [29]. Therein, we studied the effect of high-pressure vs low-pressure processing on the porosity and diffusion characteristics of LLDPE-pine flour composites. In this paper, the models of Duan [30] and of Alter [31] are used to establish the correlation of V_P with gas transport.

Thus, a holistic view of rotomolded composite materials with insights on the thermomechanical (long and short term, static and dynamic under both wet and dry conditions), microstructural and transport properties are developed in this paper.

Materials and methods

Rotomolding grade LLDPE with brand name: Alkatuff LL710UV and melt flow index (MFI) of 10 g/min was provided by Price Plastics Pty. Ltd., Dandenong, Victoria. Untreated fine pine flour was purchased from Pollard's Sawdust Supplies Pty. Ltd., Plenty, Victoria. Oak flour was sourced from Bordeaux, France. Scanning Electron Microscopy (SEM) analysis of the samples was done on a Zeiss Supra 40 Vp electron microscope. The samples analysed via SEM were first coated with gold on an Emitech K975X sputtering unit. SEM images of the raw material samples are shown in Fig. 1. Rotomolding was carried out at Roto Industries Pty. Ltd., Pakenham, Victoria and the rotomolded samples are shown in Fig. 2. The processing cycle details are in Table 2 and the compositions are shown in Table 3. Optimization of the rotomolding cycle including temperature and cycle times has been shown in our previous work [19].

For each test mentioned herewith, a minimum of 3 samples were analysed per composition to provides statistical data. Visual characteristics of the raw materials and molded samples were observed using an Olympus BX61 Optical Microscope. The crystallinity of all the molded specimens was tested using a TA DSC 2010 Differential Scanning Calorimeter. Heating runs were conducted from room temperature to 250 °C at a heating rates of 5, 10 and 15 °C/min to check the trends in and the effect of heating rate on the % crystallinity of the composite specimens. The % crystallinity of the specimen was determined using 293.1 J/g as the standard heat of fusion for 100% crystalline polyethylene [32].

The molded specimens were cut into standard dimensions for testing the mechanical properties of the manufactured composites. Tensile and flexural testing was done on a Zwick Z010 Universal testing machine with a 10 kN load cell. Tensile testing was conducted per ASTM D638 and flexural testing per ASTM D790. Izod Impact tests per ASTM D256 were done on a CEAST Impact testing machine with the notch on the sample being made on an Instron notch cutter. The results from tensile, flexural and impact testing would establish the trends in static mechanical properties of the fabricated composites independent of time and inertial effects.

Dynamic testing was then conducted on a TA Dynamic Mechanical Analyzer DMA 2980. Trends in properties obtained from dynamic testing would indicate how the fabricated composite product would perform in real life operation conditions. This included measuring the storage moduli of the samples in tensile and single cantilever modes before and after ethanol contact. A testing span of 17.5 mm was used in single cantilever mode. The frequency used was 1 Hz and the analysis was carried out from 30 °C to 100 °C at a heating rate of 3 °C/min. Creep analysis of the specimens was also done in tensile mode, before and after ethanol contact, over a period of 24 h under a stress of 1 MPa. Equilibrium compliance values (J_{eq}) from using the DMA set up in tensile mode was then converted to the corresponding equilibrium modulus values using Eq. (1).

$$E_{eq} = \frac{1}{J_{eq}} \tag{1}$$

In our previous work [29], the Burger model was used to provide the fit to the compliance data. Burger's model, shown

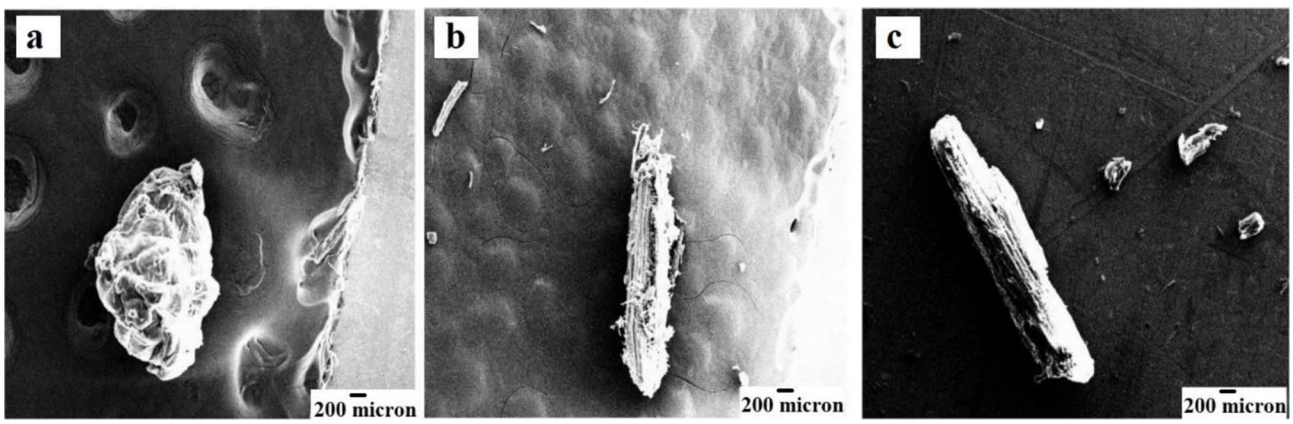

Fig. 1 SEM images of the raw materials (**a**): LLDPE, (**b**): Pine flour, (**c**): Oak flour

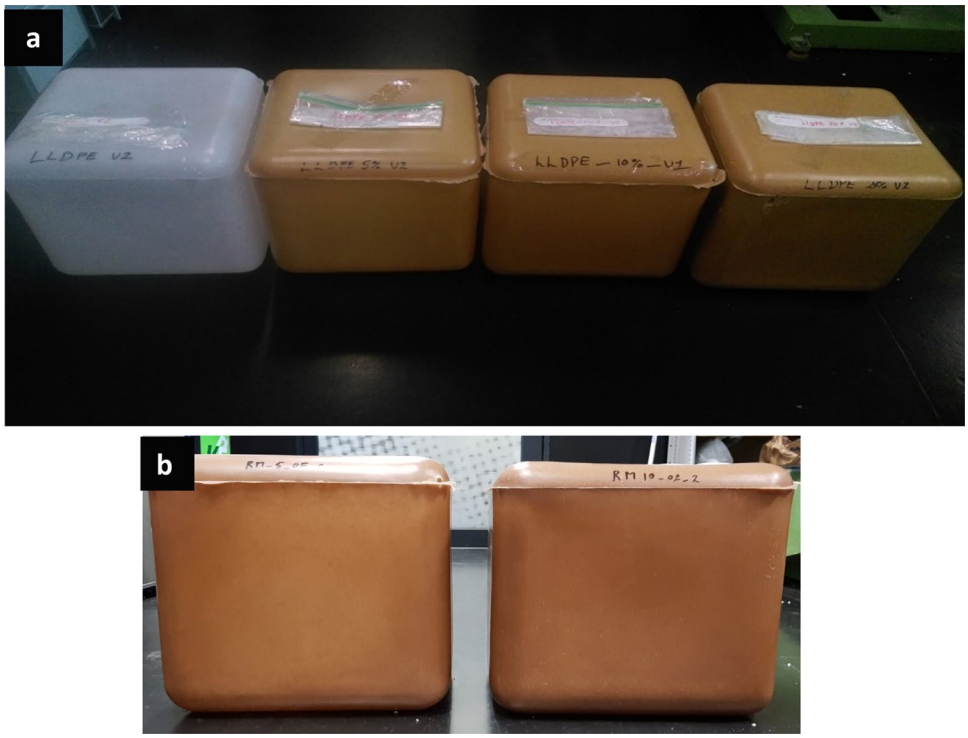

Fig. 2 (**a**): Rotomolded specimens with pine flour L-R: 0%, 5%, 10% and 20% by weight pine flour (**b**): Rotomolded specimens 5% and 10% by weight of oak flour

in Eq. (2) and Fig. 3, is a parallel combination of an elastic Maxwell element (with characteristic modulus E_M and visocosity η_M) with a viscous Kelvin Voigt element with characteristic modulus E_K and visocosity η_K). The model displays a lagging elastic response to stress represented by a relaxation time (t_r). Mathematically speaking, t_r is the time required for the strain of a suddenly strained substance to reduce to 1/e of its initial value. In [29], comparisions between the compression molded and rotomolded LLDPE pine (softwood) flour composites was done. Comparing the trends in creep compliance and E_M, the RM10 sample was found to be optimal. Expanding upon [29] in this paper, similar work was done for LLDPE oak (hardwood) flour composite but the focus was on purely rotomolded composite behaviour. To this end, some of the data from [29] (specifically, the compliance curves, E_M and η_M data for RM0 and RM10 for RM0 and RM10 in dry and wet conditions) is reproduced here to provide context. More detail on the creep modelling is also presetnted in the form of trends in E_K and t_r.

$$J(t) = \frac{1}{E_M} + \frac{1}{E_K}\left(1 - e^{\frac{-t}{t_r}}\right) + \frac{t}{\eta_M} \quad (2)$$

In order to correlate the trends in microstructural porosity to gas transport, oxygen permeability of the samples was tested on a MOCON OxTran 2/21 Oxygen Permeability Tester at Gunn Labs, Black Rock, Victoria. The analysis was carried out at 23 °C, 0% Relative Humidity (RH) under ASTM F1927. This, in combination with the ethanol transport trends in rotomolded composites detailed in [29], would provide a complete picture of the transport characteristics of the polymer natural fibre composites fabricated in this work.

Table 2 Process cycle time and other parameters of the rotomolding technique. Optimized from [19]

Cycle	RPM	Temperature (°C)	Time (min)
Heating	Major axis: 7.5, Minor axis: 5	240	12
Ambient cooling	-	Room temperature	4
Fan cooling	-	Room temperature	6
Cooling chamber	-	13	12

Table 3 Samples made from each molding method with wood flour content

Sample	Type of Wood	Wood flour content (weight %)
RM0	None	0
RM5	Pine	5
RM10	Pine	10
RM20	Pine	20
RM5_O	Oak	5
RM10_O	Oak	10

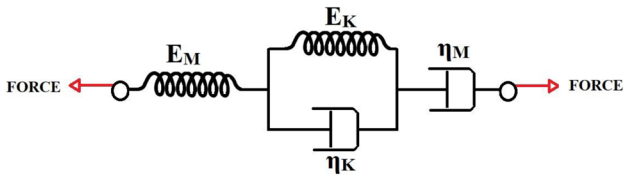

Fig. 3 Burger's representation of a viscoelastic material

Results and discussion

The flexural strengths as a function of oak and pine flour content are shown in Fig. 4a. It can be seen that there is a consistent drop with wood flour content irrespective of pine or oak. This suggests that if any potential application for this composite material is to be had, there has to be an external strengthening of the molded shape, maybe, in the form of an external scaffold. The trends in flexural strength as a function of ethanol uptake is shown in. It can be seen that with the incorporation of 5% by weight of wood flour, the flexural strength is found to reduce by 5% for the RM5 sample and by 17% for the RM5_O. The trends in 10% incorporation is a lot more pronounced with RM10 showing a 30% drop and RM10_O shows a 45% drop respectively as compared to RM0. The overall flexural strength comes into play when considering the stacking of these storage containers and therefore, it is important that a proper choice of dispersed phase concentration is done. It has to be noted that the flexural strength is maintained before and after the ethanol sorption at different temperatures (Fig. 4b). Thus, when considering alcohol-based food contact applications, the sorption of the food product into the pores of the designed storage will not have any major detriment on the mechanical performance of the unit. However, the relative drop with respect to the plain rotomolded LLDPE necessitates the use of external support structures to maintain structural integrity for any potential storage unit application. Also, for every composition, the oak flour composite has a lower flexural strength value as compared to the pine flour composite. This could be because on average, the oak flour particles are harder than the pine flour particles and therefore, harder to disperse effectively, leading to poorer mechanical performance.

The trends in storage modulus in single cantilever mode as a function of wood flour content are shown in Fig. 5a and the effect of ethanol uptake on the storage modulus are shown in Fig. 5b. Overall, there is a drop in storage modulus with increasing wood flour content similar to the trends in Fig. 5a. At 5% incorporartion of both oak and pine flour, the drop in storage modulus compared to RM0 is about 4% for RM5 and 6% for RM5_O. Following that, post ethanol uptake the RM0 sample shows an minor drop of about 2.5% while the RM5 and RM5_O samples show a drop of 2.7%

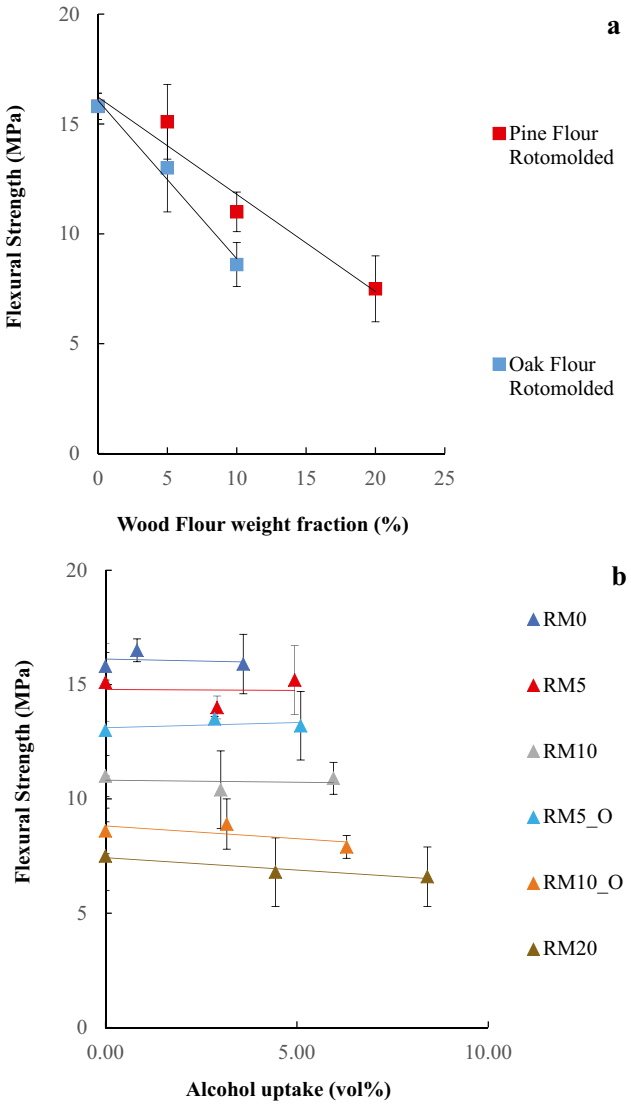

Fig. 4 Trends in flexural strength of the rotomolded LLDPE wood flour composites (**a**): as a function of wood flour content, (**b**): as a function of ethanol uptake

and 4.2% respectively. For the 10% samples, both RM10 and RM10_O show a drop of 10% in the storage modulus values post ethanol contact. The effect of ethanol uptake on the structural integrity of the composite is most apparent for the 20% sample (RM20) where post ethanol uptake at 30 °C the storage modulus drops to almost half of the modulus value under dry conditions.

The tensile strengths of the dry rotomolded samples are shown in Fig. 6. It can be seen that the tensile properties reduce consistently with wood flour incorporation irrespective of type in the rotomolded system. This indicates that the fibrous nature of the dispersed phase does not provide much reinforcement (Fig. 6a). This is because of the lower dispersive power of the rotomolding process and the interfacial

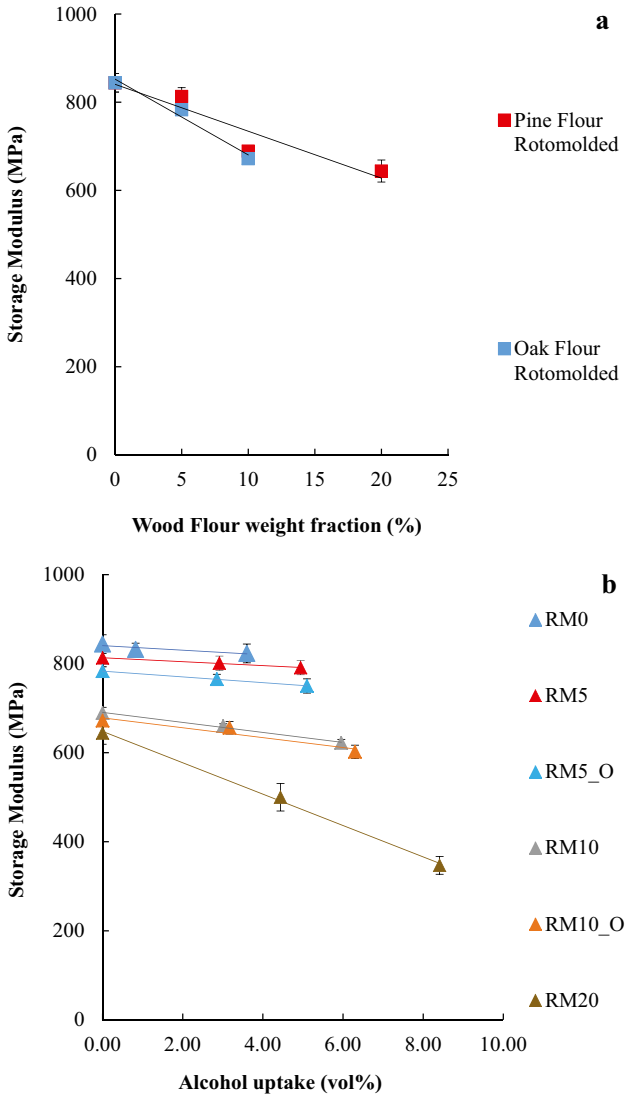

Fig. 5 Trends in storage modulus in single cantilever mode of the rotomolded LLDPE wood flour composites (**a**): as a function of wood flour content, (**b**): as a function of ethanol uptake

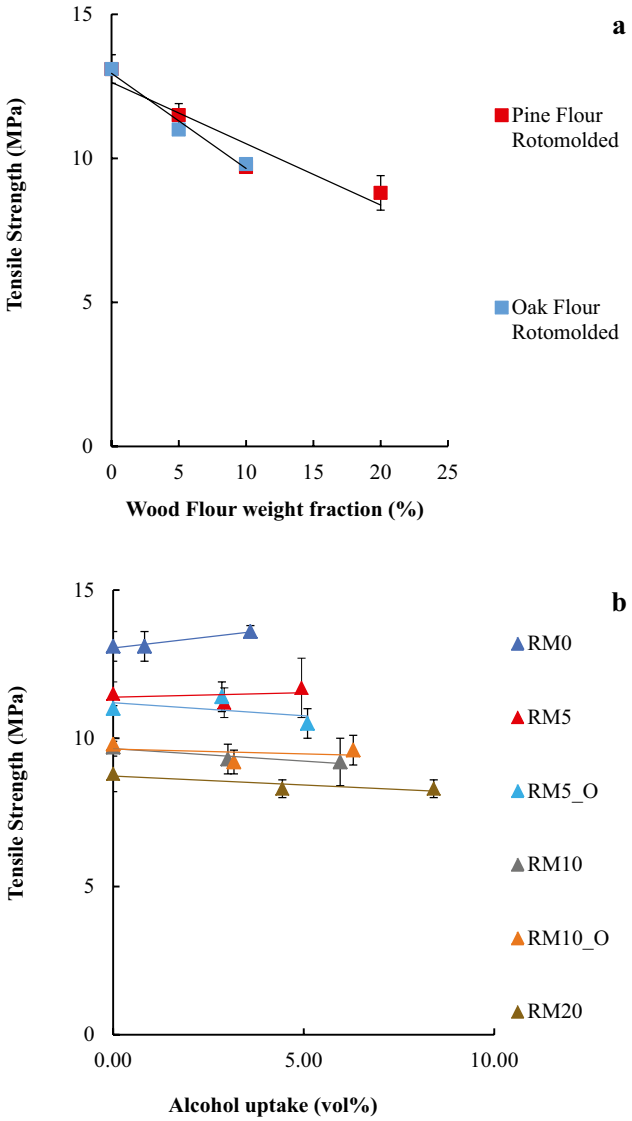

Fig. 6 Trends in tensile strength of the rotomolded LLDPE wood flour composites (**a**): as a function of wood flour content, (**b**): as a function of ethanol uptake

tension existing between the untreated fibre dispersed phase and the matrix LLDPE phase. The tensile strengths reduce by about 10% at 5% wood flour (oak or pine) incorporation and up to 30% at 10% wood flour incorporation. The trends in tensile strength as a function of ethanol uptake are shown in Fig. 6b. First and foremost, is that with an increase in the wood flour concentration, the tensile strength starts reducing with the RM10 and RM10_O samples showing tensile strengths of 9.7 ± 0.2 MPa and 9.8 ± 0.2 MPa as compared to the RM0 value of 13.1 ± 0.5 MPa. The reasons for this are clearly the lower dispersive efficiency of the rotomolding process. That being said, it is very possible that this lower dispersive efficiency can be exacerbated in the presence of sorbed ethanol. Evidence of this, however, is not seen amongst the RM5, RM10, RM20, RM5_O, RM10_O specimens. On average the overall tensile strength of the specimens is maintained after ethanol sorption and in the RM0 specimen, there is a slight increase after ethanol sorption at 30 °C. But this supposed increase is only of the order of 3% so could be attributed to experimental variation rather than a true increase in tensile strength via plasticization.

No major differences are seen in the storage modulus value in tensile mode amongst the samples containing 0, 5% and 10% by weight of wood flour (pine or oak), with the overall variation being of the order of around 2%. This indicates that the low dispersive effects of rotomolding and interfacial tension existing on account of non-compatibilization does not adversely affect the properties of the composite in tensile mode. When it comes to the effect of ethanol sorption

on the tensile storage modulus shown in Fig. 7b, it is seen that there is a formation of a band of results between ~ 500 and 550 MPa for all the samples except for RM20. This indicates that below the 20% by weight incorporation of the wood flour, no major effect of ethanol uptake is seen on the overall storage modulus. Therefore, except for RM20, all the samples maintain their tensile mechanical performances in the presence or absence of ethanol. With RM20, there is a pronounced reduction in the modulus value. For an ethanol uptake of about 8% by weight at equilibrium, there is a 23% drop in storage modulus (415 ± 30 MPa) as compared to RM0 (534 ± 20 MPa). This is also reflected in the slopes of the linear fits of the storage moduli. The RM20 specimen shows an ~ 13 times larger rate of drop of modulus value with ethanol sorption as the RM0 and a 4–11 times larger rate of drop than the specimens with 5% wood flour incorporation. Thus, with an increase in wood flour content in the rotomolded system there is a more pronounced drop in mechanical performance. This, once again, indicates that, the dispersed phase concentration needs to be ≤ 5% by weight (pine or oak). In general, the trends in storage modulus via DMA (Figs. 5a, 7a) indicated a decreasing trend as a function of wood flour content. This, in combination with the fact that our composite system is non-compatibilized system fabricated using a low pressure processing technique indicates a weak interaction between the fibre and matrix. In our previous work [19], with high pressure compression molding (which induced large shear rates), there was a

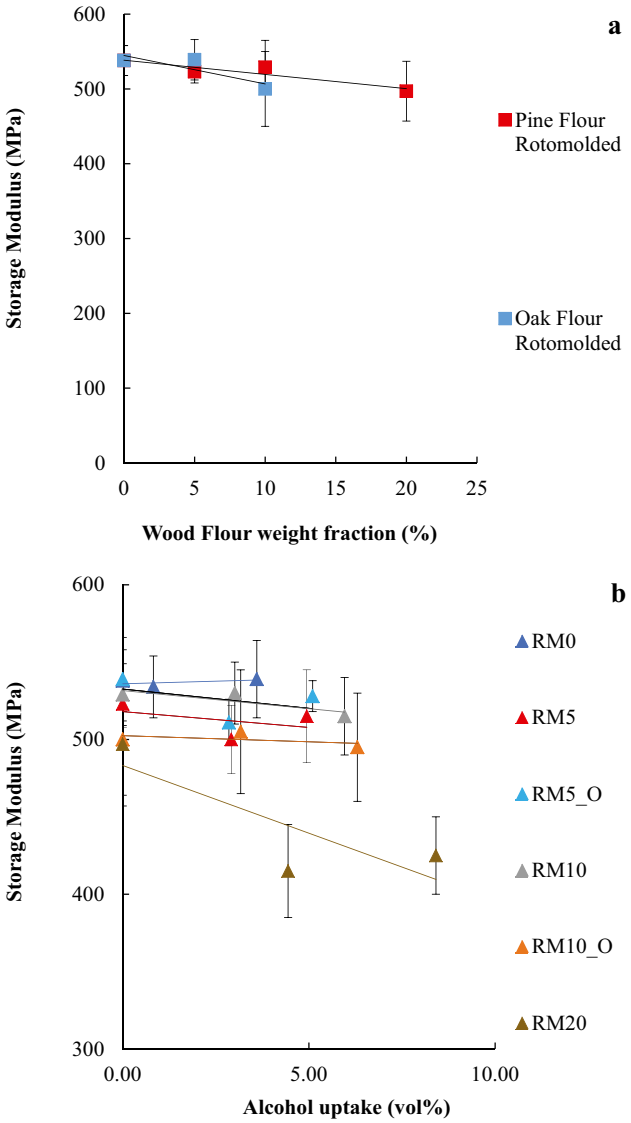

Fig. 7 Trends in storage modulus in tensile mode of the rotomolded LLDPE wood flour composites (**a**): as a function of wood flour content, (**b**): as a function of ethanol uptake

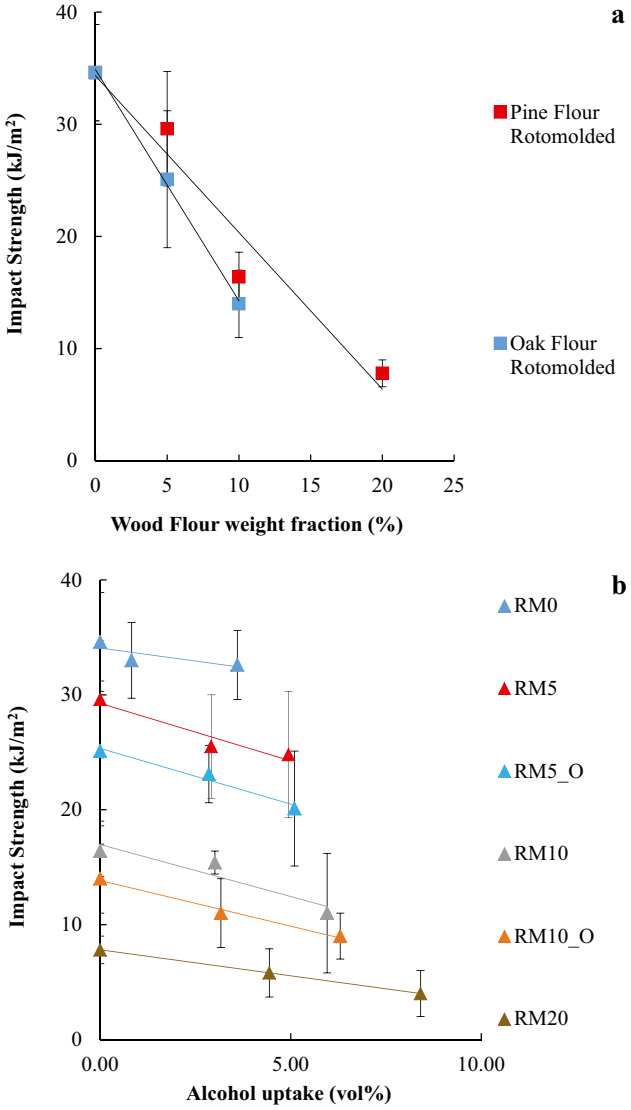

Fig. 8 Trends in impact strength of the rotomolded LLDPE wood flour composites (**a**): as a function of wood flour content, (**b**): as a function of ethanol uptake

marked increase in storage modulus indicating a relatively stronger fibre/matrix interaction.

The impact strengths of the rotomolded samples are shown in Fig. 8a. As seen for the tensile and flexural strengths, there is a clear reducing trend. The incorporation of solid fillers without any sort of compatibilization between the matrix and the dispersed phase can lead to delamination and poor interfacial properties [32]. This can have an adverse effect on the ability of the composite specimens to absorb impact and is demonstrated conclusively by the reducing trend in impact strength with increase in wood flour content. The drop in impact strength with oak flour is a lot more pronounced as compared to pine flour owing to the hardwood nature of the oak flour. With ethanol sorption, there is a further reduction in impact strength, but the reduction is not very pronounced for the RM0 specimen. For all composite specimens the drop in impact strength with ethanol sorption happens at a rate that is roughly twice the rate seen with RM0.

The trends in creep compliance for the rotomolded composites pre and post ethanol contact are shown in Fig. 9. Using the trends in Fig. 9 and applying Eq. (1), the equilibrium modulus (E_{eq}) can be estimated and the trends in E_{eq} as a function of ethanol uptake are shown in Fig. 10.

Amongst the rotomolded composites, similar negative slopes are seen for the E_{eq} modulus values with increase ethanol content (Fig. 10). This can be attributed to a combination of the low dispersive effects of rotomolding and the sintering-based formation mechanism of the rotomolded composites. Images that display this sintering-based mechanism for the rotomolded LLDPE pine flour composites have been shown in our previous works [19, 29]. Images of the sintering mechanism and formation of RM5_O and RM10_O are shown in Fig. 11a, b respectively. It was observed that optical microscopy was able to provide the resolution required to make appropriate inferences for our work. However, more detail can be observed through SEM analysis and for this the reader can refer to microstructural SEM data shown in our previous

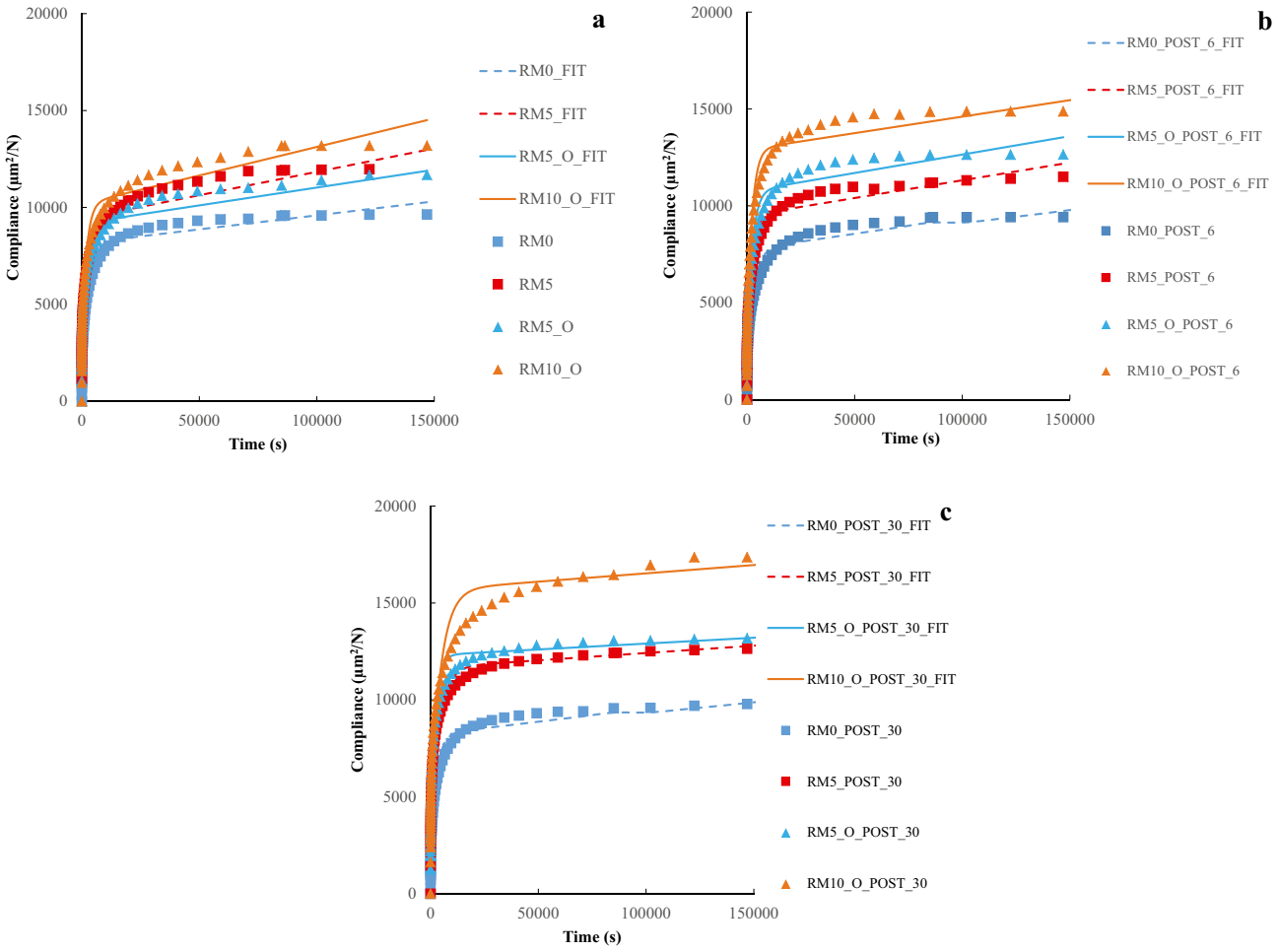

Fig. 9 Creep compliance rotomolded LLDPE wood flour composites (**a**): dry, (**b**): post ethanol uptake at 6 °C, (**c**): post ethanol uptake at 30 °C. Data for RM0 and RM5 has been reproduced with permission from our previous work [29]

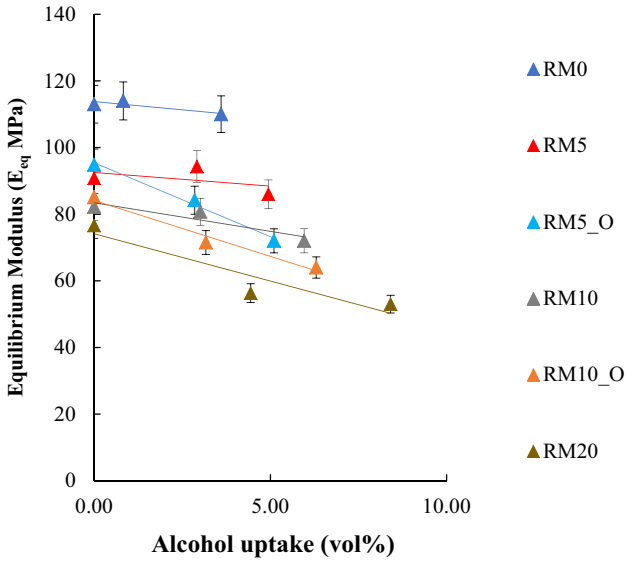

Fig. 10 Equilibrium Modulus vs ethanol uptake of the rotomolded LLDPE wood flour composite samples

work [19]. Therein, a significant porosity is observed in the microstructure of fractured impact tested samples attributed to the uncompatibilized nature of the rotomolded composites. As far as the sintering mechanism is concerned, the evolution is very similar to the ones observed in Fig. 3 of [29]. Thus, for the rotomolded composites, it must be acknowledged that beyond a loading of 10% by weight of the wood flour phase, the reduction in the modulus values are quite unsustainable and in reality, for uncompatibilized composites like the ones studied in this paper, the optimized composition is closer to 5%.

In our previous paper [29], we have shown how to fit Burger's viscoelastic material to model the creep behaviour and estimated the Maxwell modulus (E_M) and the Maxwell viscosity (η_M) for the rotomolded LLDPE pine flour composites. It was observed in [29] that with the use of pine flour in the rotomolded material, the E_M values reduce compared to RM0 (296 MPa). RM5 has an E_M that is 24% lower (226 MPa) than that of RM0 and further addition of pine flour for RM10 and RM20 ends up producing composites with E_M values that are 27% (217 MPa) and 29% (209 MPa) respectively lower than that of RM0. For the rotomolded oak composites studied in this work, the E_M values of RM5_O and RM10_O were found to be 215 MPa and 200 MPa respectively indicating that the hardwood oak flour composite stiffness was reducing at a larger rate than the softwood pine flour composites. Expanding on that work, we have now estimated the Kelvin Voigt moduli and relaxation times of the creep behaviour of both LLDPE pine and LLDPE oak flour composites. The second set of results obtained from fitting Burger's model are related to the Kelvin Voigt modulus and the relaxation time. Both parameters are associated with the amorphous part of a semi-crystalline polymer. The trends in E_K as a function of wood flour content are shown in Fig. 12a and it can be seen that at 5% wood flour incorporation, the values are quite similar to that of RM0 but reduce consistently at higher wood flour weight fractions. As far as the effect of the ethanol sorption, irrespective of composition or the type of dispersed phase there is a drop in E_K values post sorption as compared to the E_K pre sorption (Fig. 12b). This drop is due to the slight plasticizing effect of the sorbed ethanol and is more obvious amongst the wood flour composites than with the plain polymer because of the hydrophilic nature of both dispersed phases and the permeant.

The t_r values (Fig. 12c), for the most part, show a reducing trend with increasing ethanol contact. This again speaks to the plasticizing nature of the ethanol for the system. The only samples this is not seen for is the samples without any wood flour incorporation ie RM0. Therefore, the plasticizing effect of ethanol uptake in our system can only be observed in the presence of the filler material.

Based on the results in dynamic properties and the trends thereof as a function of wood flour concentration and ethanol uptake, an understanding of the maximum loading of wood flour before a general downtrend in mechanical performance begins has been established. For the rotomolding process, it can be stated that that optimal concentration is 5% by weight of wood flour, both independent of the type of wood flour used.

It is well known that intensive properties such as crystallinity and density of a polymer significantly influence the overall permeation characteristics [30]. However, models developed on this basis are not completely deterministic in nature because they often include parameters that are customised to individual systems [33]. One such model that correlates crystallinity to polymer permeability is the one by Duan et al. [30] shown in Eq. (3).

$$P = P_C\left(\frac{1 - X_c}{1 + 0.5X_c}\right) \tag{3}$$

Here, Xc refers to the fractional degree of crystallinity. The logic behind the development of this model is that while a linear model would show zero permeability at < 100% crystallinity, this particular model shows zero permeability at exactly 100% crystallinity. In order to estimate the differences in crystallinity between the different composites, Differential Scanning Calorimetry (DSC) was carried out. The area under the melting curve was estimated from the DSC graph and using the heat of fusion for purely crystalline PE which is 293.1 J/g [32]. Based on this, the % crystallinities of all the composite specimens and the raw material LL710UV are shown in Table 4.

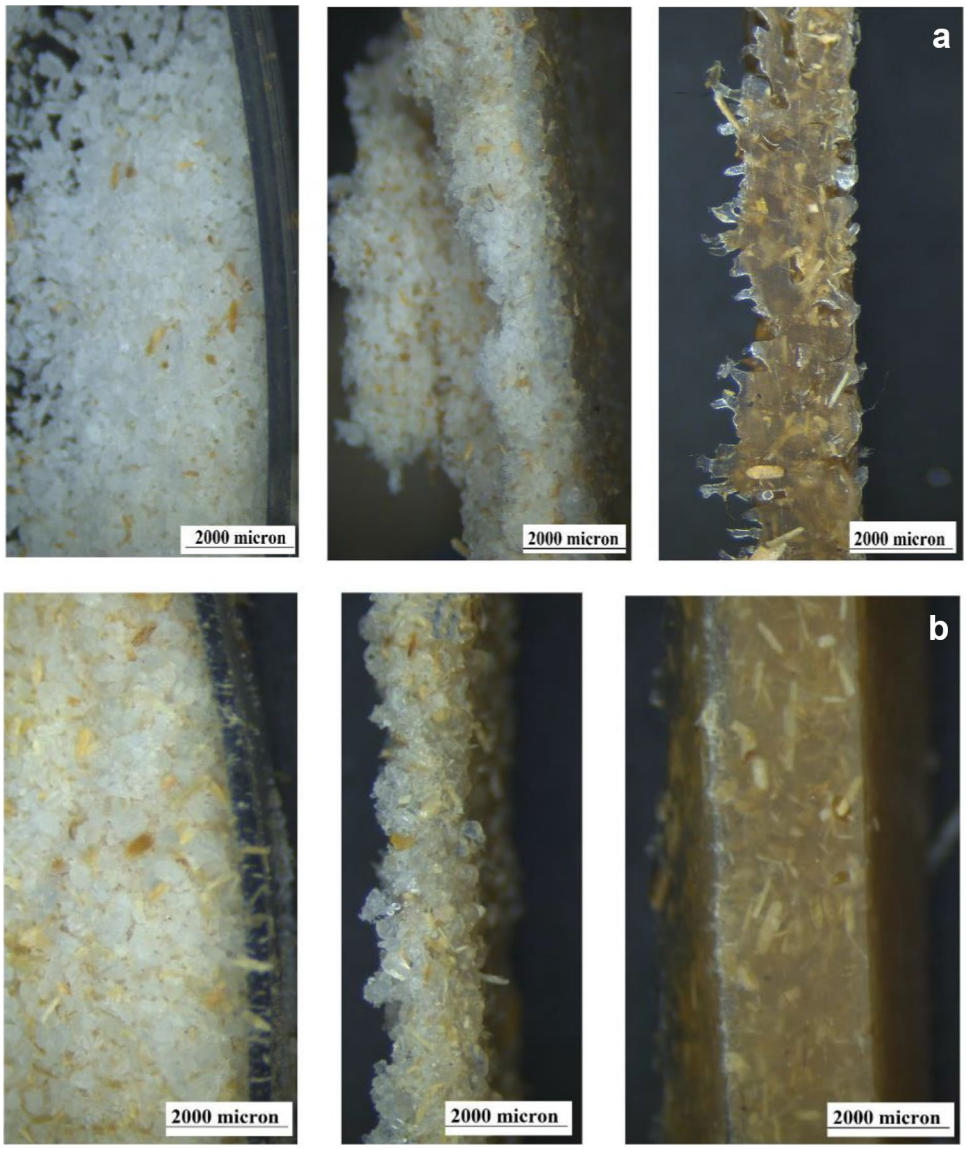

Fig. 11 Evolution of microstructure in LLDPE raw material with wood flour (L-R) 200 °C, 5 min; 200 °C, 10 min; 240 °C at 12 min for (**a**): 5% oak flour, (**b**): 10% oak flour

From Table 4, it can be seen that there are no major differences or trends in % crystallinity values. Therefore, this result combined with the results in Prasad et al. [34], who suggest that the diffusion coefficient and thus, permeability of a perfectly crystalline polymer may be a non-zero value, means that other intensive properties are needed to effectively model polymer permeability. The trends in V_P estimated in [29] indicate an increased porous microstructure for the rotomolded composites with wood flour incorporation. Hence, to confirm whether these trends also correlated with increased O_2 permeabilities, gas permeability testing of the RM0, RM5_O and RM10_O samples was carried out. The values are shown in Table 5 and the trends were fit using the Alter model [31] in Fig. 13. The Alter model is another expression that correlates an intensive property (in this case, density or 'ρ') to polymer permeability [31]. The model expression is shown in Eq. (4) and is based on the observation that density is a parameter that can help correlate subtle differences between different areas of the polymer sample to its overall permeability.

$$P = K(1-\rho)^n \quad (4)$$

Based on Fig. 13, it is possible to state the model equations for oxygen permeability (P_{pred}) of the rotomolded composites. The model equation for the pine and oak composites is shown in Eq. (5) and Eq. (6) respectively.

$$P_{Pine} = 9.1 \times 10^4 \times (1-\rho)^{0.43} \quad (5)$$

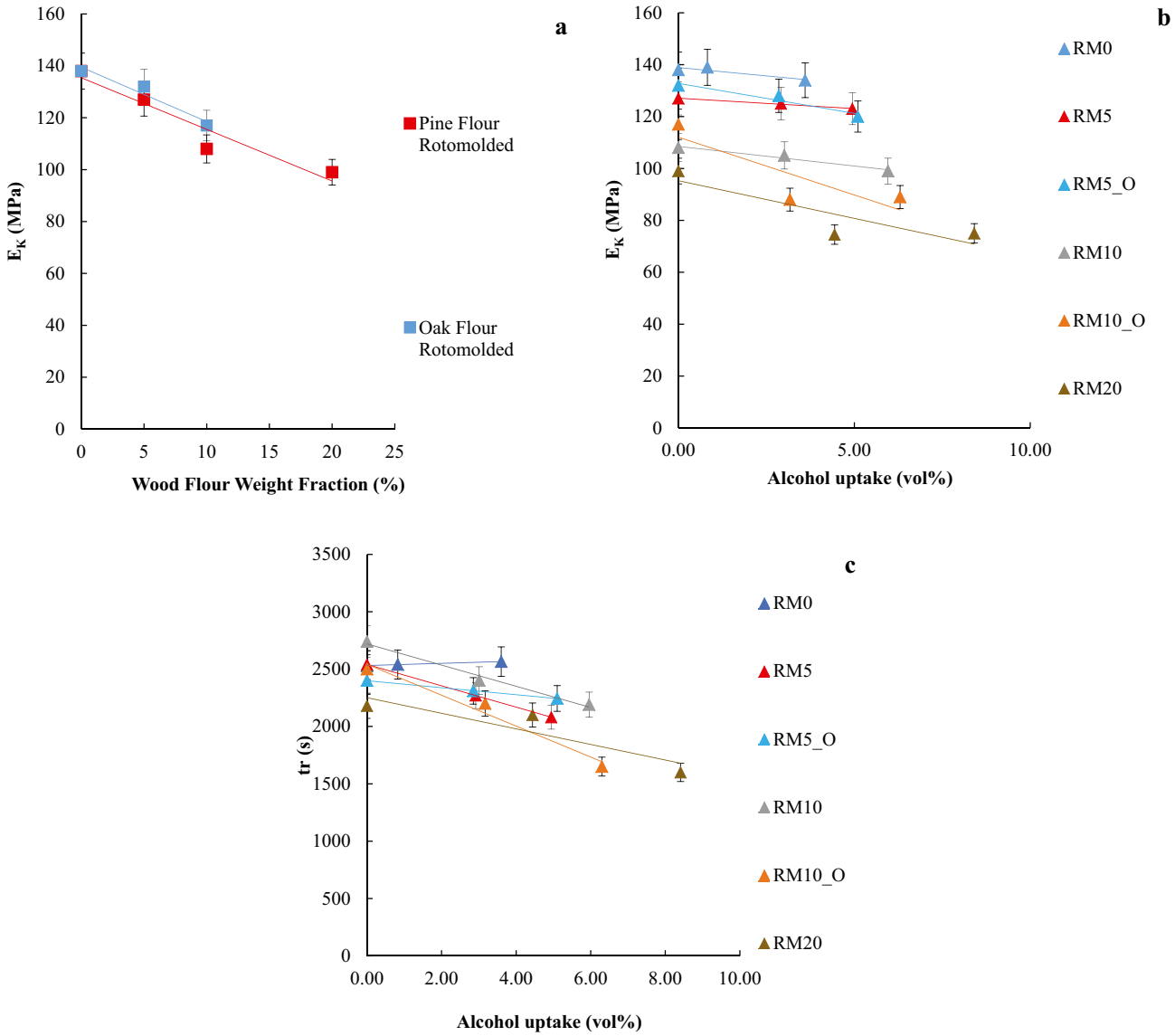

Fig. 12 Burger model parameters of the rotomolded LLDPE wood flour composite samples (**a**): Kevin Voigt modulus vs wood flour content (**b**): Kelvin Voigt Modulus vs ethanol uptake, (**c**): Relaxation time vs ethanol uptake

Table 4 % Crystallinities of all samples at 3 different heating rates.

Sample	X_C		
	5 °C/min	10 °C/min	15 °C/min
Raw material LL710UV	48.8	46.1	47.0
RM0	44.4	47.8	45.4
RM5	51.5	46.7	48.5
RM10	45.4	45.4	49.1
RM20	49.8	44.8	49.8
RM5_O	48.1	49.1	46.7
RM10_O	50.6	46.7	44.4

Table 5 Experimental (Pexp) vs predicted (Ppred) oxygen permeability values of rotomolded composites

Sample	ρ (g/cm^3)	P experimental ($cm^3.mm/m^2/year$)	P predicted ($cm^3.mm/m^2/year$)
RM0	0.93	28,616 ± 716	31,065
RM5	0.90	34,592 ± 1534	35,829
RM10	0.86	38,544 ± 658	40,991
RM5_O	0.89	38,835 ± 3407	34,326
RM10_O	0.84	39,712 ± 2500	41,336

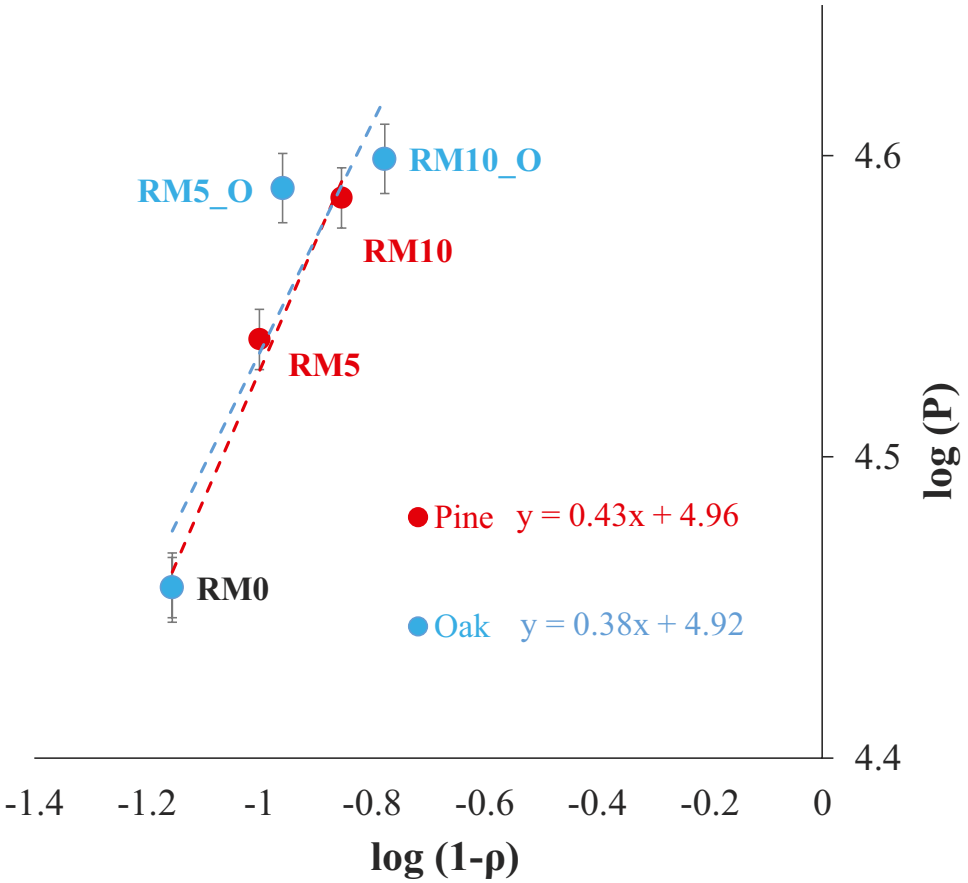

Fig. 13 Oxygen Permeability of all rotomolded composites

$$P_{Oak} = 8.3 \times 10^4 \times (1-\rho)^{0.38} \quad (6)$$

Thus, the composites do not differ noticeably in terms of crystallinity but do in terms of density. In terms of gas transport, the porosity created can be directly correlated to changes in density. As density is an intensive parameter it is an effective tool for modelling this transport phenomenon. The model of Alter [21] performs quite acceptably for all rotomolded composites made studied in this paper independent of the type of dispersed phase used.

Conclusions

All static mechanical properties of the rotomolded composites (flexural, tensile and impact strengths) are found to reduce with wood flour incorporation independent of the hard or softwood nature of the dispersed phase. This is also seen with the trends in the storage moduli in tensile and cantilever modes. The reducing trends are more pronounced with increasing wood flour content and the worst performance is seen in the RM20 composite. In terms of long-term properties, the Maxwell moduli reduce by 20–30% as compared to RM0 indicating a drop in stiffness with wood flour incorporation. A 10–12% drop is seen for the Kelvin Voigt moduli indicating that there is minimal plasticizing effects with ethanol sorption. The relaxation time continuously reduces for all the composite specimens, while being relatively stable for the RM0, indicating that the ethanol sorption induced plasticizing behaviour is restricted to only the composite systems. The overall crystallinities of the specimens are consistent and therefore the model of Duan and Thomas shown in Eq. (3) is not effective in modelling gas permeability. However, the trends in V_P studied in our previous works helped correlate the overall densities to gas permeability and to this end, the model of Alter shown in Eq. (4) is found to be highly capable of predicting oxygen permeabilities of the rotomolded composites.

Funding Open Access funding enabled and organized by CAUL and its Member Institutions. Swinburne University of Technology, Swinburne University Postgraduate Research Award, K Prasad

Declarations

Conflicts of interests The authors declare no conflict of interest. KP was funded by the Swinburne University Postgraduate Research Award (SUPRA).

References

1. Crawford RJ (1996) Recent advances in the manufacture of plastic products by rotomoulding. J Mater Process Technol 56:263–271
2. Ramkumar PL, Kulkarni DM, Abhijit VVR, Cherukumudi A (2014) Investigation of Melt Flow Index and Impact Strength of Foamed LLDPE for Rotational Moulding Process. Procedia Materials Science 6:361–367
3. Ramkumar PL, Ramesh A, Alvenkar PP, Patel N (2015) Prediction of heating cycle time in Rotational Moulding. Materials Today: Proceedings 2:3212–3219
4. Rao MA, Throne JL (1972) Principles of rotational molding. Polym Eng Sci 12:237–264
5. George J, Joseph K, Bhagawan SS, Thomas S (1993) Influence of short pineapple fiber on the viscoelastic properties of low-density polyethylene. Mater Lett 18:163–170
6. George J, Bhagawan SS, Prabhakaran N, Thomas S (1995) Short pineapple-leaf-fiber-reinforced low-density polyethylene composites. J Appl Polym Sci 57:843–854
7. George J, Sreekala MS, Thomas S (2001) A review on interface modification and characterization of natural fiber reinforced plastic composites. Polym Eng Sci 41:1471–1485
8. Mohanty AK, Vivekanandhan S, Pin JM, Misra M (2018) Composites from renewable and sustainable resources: Challenges and innovations. Science 362:536–542
9. Pandey JK, Ahn SH, Lee CS, Mohanty AK, Misra M (2010) Recent Advances in the Application of Natural Fiber Based Composites. Macromol Mater Eng 295:975–989
10. Sreekala MS, Kumaran MG, Joseph S, Jacob M, Thomas S (2000) Oil Palm Fibre Reinforced Phenol Formaldehyde Composites: Influence of Fibre Surface Modifications on the Mechanical Performance. Appl Compos Mater 7:295–329
11. Balakrishnan P, John MJ, Pothen L, Sreekala MS, Thomas S (2016) Natural fibre and polymer matrix composites and their applications in aerospace engineering. In: Fangueiro R (ed) Rana S. Advanced Composite Materials for Aerospace Engineering, Woodhead Publishing, pp 365–383
12. Goda K, Sreekala MS, Gomes A, Kaji T, Ohgi J (2006) Improvement of plant based natural fibers for toughening green composites—Effect of load application during mercerization of ramie fibers. Compos A Appl Sci Manuf 37:2213–2220
13. Goda K, Cao Y (2007) Research and Development of Fully Green Composites Reinforced with Natural Fibers. J Solid Mech Mater Eng 1:1073–1084
14. Torres FG, Aragon CL (2006) Final product testing of rotational moulded natural fibre-reinforced polyethylene. Polym Testing 25:568–577
15. Wang B, Panigrahi S, Tabil L, Crerar W (2007) Pre-treatment of Flax Fibers for use in Rotationally Molded Biocomposites. J Reinf Plast Compos 26:447–463
16. López-Bañuelos RH, Moscoso FJ, Ortega-Gudiño P, Mendizabal E, Rodrigue D, González-Núñez R (2012) Rotational molding of polyethylene composites based on agave fibers. Polym Eng Sci 52:2489–2497
17. Torres F, Aguirre M (2003) Rotational Moulding and Powder Processing of Natural Fibre Reinforced Thermoplastics. Int Polym Proc 18:204–210
18. Hanana FE, Chimeni DY, Rodrigue D (2018) Morphology and Mechanical Properties of Maple Reinforced LLDPE Produced by Rotational Moulding: Effect of Fibre Content and Surface Treatment. Polym Polym Compos 26:299–308
19. Prasad K, Nikzad M, Doherty C, Sbarski I (2019) Predicting trends in structural and physical properties of a model polymer with embedded natural fibers: Viability of molecular dynamics studies for a bottom up design. J Appl Polym Sci 136:48189
20. González-López ME, Pérez-Fonseca AA, Cisneros-López EO, Manríquez-González R, Ramírez-Arreola DE (2019) Effect of Maleated PLA on the Properties of Rotomolded PLA-Agave Fiber Biocomposites. J Polym Environ 27:61–73
21. Ortega Z, Monzón MD, Benítez AN, Kearns M, McCourt M, Hornsby PR (2013) Banana and Abaca Fiber-Reinforced Plastic Composites Obtained by Rotational Molding Process. Mater Manuf Processes 28:879–883
22. Barczewski M, Szostak M, Nowak D, Piasecki A (2018) Effect of wood flour addition and modification of its surface on the properties of rotationally molded polypropylene composites. Polimery -Warsaw- 63:772–784
23. Greco A, Maffezzoli A (2015) Rotational molding of biodegradable composites obtained with PLA reinforced by the wooden backbone of opuntia ficus indica cladodes. J Appl Polym Sci 132:42447
24. Greco A, Maffezzoli A (2016) Rotational moulding of poly-lactic acid. AIP Conf Proc 1779:060007
25. Chandran VG, Waigaonkar S (2017) Mechanical properties and creep behavior of rotationally moldable linear low density polyethylene-fumed silica nanocomposites. Polym Compos 38:421–430
26. Sari PS, Thomas S, Spatenka P, Ghanam Z, Jenikova Z (2019) Effect of plasma modification of polyethylene on natural fibre composites prepared via rotational moulding. Compos B Eng 177:107344
27. Chandran VG, Waigaonkar S (2016) Investigations on cycle time reduction, dynamic mechanical properties and creep for rotationally moldable nano composites of linear low density polyethylene and fumed silica. Nanosystems: Phys Chem Math 609–612
28. Pozhil SN, Menon NM, Waigaonkar SD, Chaudhari V (2020) An analytical model to predict the creep behaviour of linear low-density polyethylene (LLDPE) and polypropylene (PP) used in rotational moulding. Materials Today: Proceedings 28:888–892
29. Prasad K, Nikzad M, Sbarski I (2020) Using viscoelastic modeling and molecular dynamics based simulations to characterize polymer natural fiber composites. J Appl Polym Sci 137:49220
30. Duan Z, Thomas NL (2014). Water vapour permeability of poly(lactic acid): Crystallinity and the tortuous path model. J Appl Phys 115:064903
31. Alter H (1962) A critical investigation of polyethylene gas permeability. J Polym Sci 57:925–935
32. Al-Jabareen A, Al-Bustami H, Harel H, Marom G (2013) Improving the oxygen barrier properties of polyethylene terephthalate by graphite nanoplatelets. J Appl Polym Sci 128:1534–1539
33. Prasad K, Nikzad M, Sbarski I (2021) Modeling Permeability in Multi-Phase Polymer Composites: A Critical Review of Semi-Empirical Approaches. Polym Rev 61:194–223
34. Prasad K, Nikzad M, Doherty C, Sbarski I (2018) Diffusion of low-molecular-weight permeants through semi-crystalline polymers: combining molecular dynamics with semi-empirical models. Polym Int 67:717–725